

Structural and Functional Analyses of Benzamidine-Based Inhibitors in Complex with Trypsin: Implications for the Inhibition of Factor Xa, tPA, and Urokinase

Martin Renatus,^{†,||} Wolfram Bode,[†] Robert Huber,[†] Jörg Stürzebecher,[‡] and Milton T. Stubbs^{*,†,§}

Max-Planck-Institut für Biochemie, Abteilung Strukturforschung, Am Klopferspitz 18a, D-82152 Martinsried, Germany, Klinikum der Friedrich-Schiller-Universität Jena, Zentrum für Vaskuläre Biologie und Medizin, Nordhäuser Str. 78, D-99089 Erfurt, Germany, and Institut für Pharmazeutische Chemie der Philipps-Universität Marburg, Marbacher Weg 6, D-35032 Marburg, Germany

Received August 5, 1998

The trypsin-like serine proteinase superfamily contains a number of potential therapeutic targets, many of which are unsuitable for routine X-ray crystallographic studies. We have cocrystallized a selection of benzamidine-based inhibitors with bovine trypsin and solved their structures to a resolution of up to 1.7 Å. Despite similar chemical formulas, the inhibitors exhibit a range of diverse binding modes that reflect their inhibitory spectra against the serine proteinases trypsin, thrombin, factor Xa, tissue-type plasminogen activator (tPA) and urokinase (uPA). In contrast to the compact folded conformations of thrombin inhibitors which allow optimal binding in the well-defined hydrophobic S2/S4 pocket of thrombin, those effective against factor Xa exhibit an extended conformation that allows occupation of the S3/S4 region, where hydrophobic and electrostatic interactions can stabilize the conformation. One group of inhibitors containing an N-terminal 2,4,6-triisopropylphenylsulfonyle (TIPPS) moiety show little or no penetration into the S3/S4 subsites of trypsin. These latter sites are occluded in uPA, explaining why this class of compounds is effective against uPA. Despite presenting an extensive hydrophobic surface toward the solvent, the K_i values for TIPPS-containing compounds against trypsin is in the range 10^{-7} to 10^{-8} M. Comparison of the binding of a bis-benzamidine inhibitor in trypsin and tPA indicate that a shift in potency can be induced by relatively minor changes in binding mode. Implications for the inhibition of these proteinases are discussed.

Introduction

Trypsin-like serine proteinases play a central role in a wide range of biological processes, many of which can lead to pathological conditions. Their regulation is therefore an attractive target for potential therapies. Most notably, the blood coagulation cascade is rich in such proteinases, including the procoagulant enzymes thrombin, factor Xa, factor IXa, factor VIIa, the anti-coagulant activated protein C, and the fibrinolytic enzymes plasmin and its activators tPA and uPA.¹ Furthermore, uPA plays a role in tumor metastasis and invasion. Suitable selective inhibitors of such proteinases could result in useful therapeutics for, e.g., thrombosis² or cancer.^{3,4}

Over the last 30 years, we have constructed a library of benzamidine-based compounds and tested them against a range of trypsin-like serine proteinases to obtain structure–activity relationships (SARs).^{5–8} Despite similar chemical structures (Figure 1), the compounds vary widely in their specificity and selectivity for different serine proteinases (Table 1). The inhibitors

can be grouped to a certain extent into functional classes, e.g. thrombin, factor Xa, or uPA inhibitors. In the absence of three-dimensional structural information, these SARs have proved difficult to rationalize.⁹

The three-dimensional structure determination of human α -thrombin¹⁰ opened the door to structure-based design of inhibitors as potential antithrombotic drugs¹¹ and is being used increasingly for the design and optimization of novel leads. The case of thrombin is particularly instructive. The first crystal structure of thrombin solved¹⁰ included the covalently bound inhibitor D-Phe-Pro-Arg-chloromethyl ketone and was therefore not amenable to the soaking of noncovalent inhibitors. Solution of the structure of NAPAP (**1**) in complex with the archetypal serine proteinase trypsin and superposition of the trypsin moiety on thrombin^{12,13} revealed the structural grounds for the high affinity of NAPAP for thrombin, subsequently verified by X-ray cocrystallographic studies of NAPAP and thrombin.^{14,15}

Structures of a number of serine proteinases that are potential therapeutic targets are now available, including factor Xa,¹⁶ tPA¹⁷, and uPA.¹⁸ The structure determination of factor Xa¹⁶ promised to allow the inhibitor design cycle to be applied to factor Xa as a target for specific inhibitors.¹⁹ As the existing crystals of factor Xa were unsuitable for inhibitor-soaking experiments,¹⁶ however, the binding mode of factor Xa specific inhibitors was investigated in the related enzyme trypsin.²⁰ The proposed binding mode was subsequently confirmed in a cocrystallization study with factor Xa.²¹ Similarly,

* Address correspondence to Milton T. Stubbs, Institut für Pharmazeutische Chemie der Philipps-Universität Marburg, Marbacher Weg 6, D-35032 Marburg, Germany. Tel: +49 6421 28 5999. Fax: +49 6421 28 8994. E-mail: stubbs@mail.uni-marburg.de.

[†] Max-Planck-Institut für Biochemie.

[‡] Klinikum der Friedrich-Schiller-Universität Jena.

[§] Institut für Pharmazeutische Chemie der Philipps-Universität Marburg.

^{||} Present address: The Burnham Institute, 10901 North Torrey Pines Road, La Jolla, CA 92037.

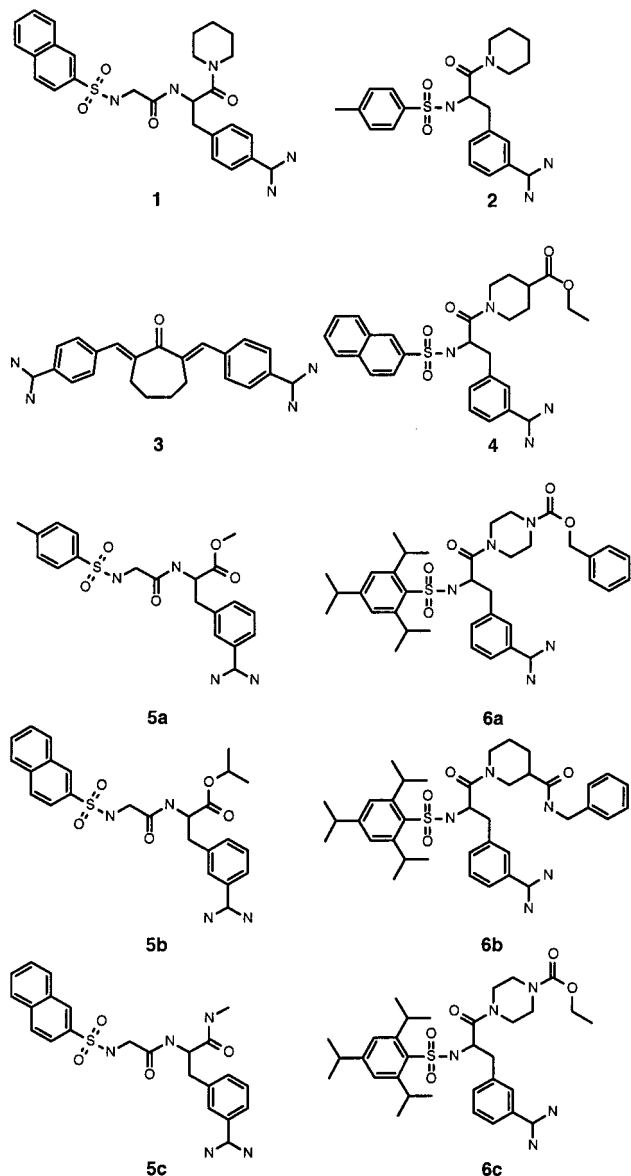


Figure 1. Chemical formulas of inhibitors used in this study.

Table 1. Dissociation Constants K_i (μM) for Inhibition of Bovine Trypsin, Bovine Thrombin, Bovine Factor Xa, Human Two-Chain tPA, and Human uPA^a

	trypsin	factor Xa	thrombin	tPA	uPA
1 (NAPAP)	0.69	7.9	0.0060	70	>1000
2 (TAPAP)	1.2	15	0.34	120	55
3	0.09	0.013	0.32	0.035	3.4
4 *	0.0084	18	0.22	24	4.5
5a	5.7	0.84	3.9	23	78
5b	3.7	0.24	1.2	33	49
5c	9.2	3.0	9.6	69	>1000
6a	0.20	2.7	1.1	0.95	1.4
6b	0.46	2.5	1.8	0.98	1.6
6c *	0.037	1.7	0.49	0.57	0.41
benzamidine	39	160	890	910	180

^a Values are for D,L-racemates except those denoted by an asterisk (*), where the pure L-enantiomer was measured.

the uPA structure published recently¹⁸ offers the possibility of understanding the specificity of uPA over related serine proteinases such as tPA on the basis of computer modeling. Despite its high sequence homology and similar substrate specificity, some important structural differences are evident. The use of the covalent inhibitor Glu-Gly-Arg-chloromethyl ketone for crystal-

lization, however, precludes the structure determination of inhibitor:uPA complexes. Until now, neither modeled nor experimental uPA:low molecular weight inhibitor complexes have been reported.

In the present study, we examine the binding modes of selected benzamidine-based inhibitors (Figure 1) in the active site of trypsin using X-ray crystallography and relate their selectivity (Table 1) to the published structures of factor Xa, tPA, and uPA.

Experimental Section

Purification of the Protein and Synthesis of the Inhibitors. Bovine β -trypsin was separated from commercial trypsin (Sigma) by ion-exchange chromatography on SP-sephadex C50.²² The inhibitors were developed and synthesized by the group of J. Stürzebecher together with the group of G. Wagner (Leipzig, Germany) and Pentapharm Ltd. (Basel, Switzerland). The inhibitors are NAPAP (**1**), 3-TAPAP (**2**), 2,7-bis(4-amidinobenzylidene)-cycloheptan-1-one (**3**), N^L -(2-naphthylsulfonyl)-3-amidino-L-phenylalanine-isonipicotic acid ethylester (**4**), N^L -tosylglycyl-3-amidino-D,L-phenylalanine-methylester (**5a**), N^L -(2-naphthylsulfonyl)glycyl-3-amidino-D,L-phenylalanine-isopropylester (**5b**), N^L -(2-naphthylsulfonyl)glycyl-3-amidino-D,L-phenylalanine-methylamide (**5c**), N^L -2,4,6-triisopropylphenylsulfonyl-3-amidino-D,L-phenylalanine-4'-benzyloxycarbonyl-piperazine (**6a**), N^L -2,4,6-triisopropylphenylsulfonyl-3-amidino-D,L-phenylalanine-nipicotic acid benzylamide (**6b**), and N^L -2,4,6-triisopropylphenylsulfonyl-3-amidino-L-phenylalanine-4'-ethoxycarbonyl-piperazine (**6c**). Synthesis and determination of K_i values have been described elsewhere; K_i values that have not yet been published were determined in the same way.⁵⁻⁸

Crystallization and Structure Analysis. All inhibitors were cocrystallized with bovine β -trypsin at room temperature using vapor diffusion. The protein concentration varied between 7 and 10 mg/mL and the inhibitor concentration between 1 and 10 mM, i.e., 5- to 20-fold molar excess. Crystals grew at slightly basic pH (7–8.5) from 0.1 to 0.3 M ammonium sulfate and 15–30% poly(ethylene glycol) 6K, with the addition of 5% methylpentanediol in some cases, mostly within 1 week. Data were collected using either a Mar Research image plate system installed on a Rigaku rotating anode generator and evaluated with MOSFLM²³ or a Centronix area detector (Siemens) and processed using XDS.²⁴ Starting coordinates were taken from the Protein Data Bank depending on the space group. Where necessary, the structures were solved using Patterson search methods with the program AMoRe²⁵ (**3E**, **6aC**, **6bC**, and **6cD**)—see Table 2 for numbering system.²⁶ Conventional crystallographic refinement (rigid body, positional, temperature factor) was carried out using XPLOR.²⁷ Molecular models of the inhibitors were constructed using SYBYL (Tripos Associates), and model building was performed using O.²⁸ Target values for bond length and angle refinement of the inhibitors were those obtained after conjugate gradient energy minimization in SYBYL; planarity constraints were applied only weakly, while all dihedral angles were left free to rotate. Data collection and refinement statistics are given in Tables 2 and 3, respectively.

Results

Inhibitor binding was investigated using cocrystallization techniques, resulting in a variety of different resolutions and crystal forms, three of which have not previously been observed (**C**, **D**, and **E**) (Table 2). In some cases, the inhibitor molecule itself contributes to crystal contacts; this will be discussed for the individual inhibitors below. To distinguish the different structures, each inhibitor is denoted by its compound number and crystal form as indicated in Table 2, e.g., **5aB** denotes the structure of inhibitor **5a** as found in crystal form **B** (orthorhombic).²⁶

Table 2. Data Collection Statistics²⁶

structure	compound	crystal form	space group	cell constants						observed/unique reflections	R_{sym}
				a (Å)	b (Å)	c (Å)	α (deg)	β (deg)	γ (deg)		
3A	3	A^b	$P3_121$	55.1	55.1	109.2	90	90	120	93904/20113	4.3%
3E	3	E^b	$C222_1$	77.0	84.3	101.5	90	90	90	44761/10118	16% at 1.75 Å 9.6% 26% at 2.35 Å
4A	4	A^b	$P3_121$	55.4	55.4	109.4	90	90	120	14708	5.3% 30.2% at 1.8 Å
5aA	5a	A^a	$P3_121$	55.1	55.1	109.1	90	90	120	77740/20294	6.9% 14.2% at 1.7 Å
5aB	5a	B^a	$P2_12_12_1$	55	58.7	67.7	90	90	90	72932/23361	5.3% 15.9% at 1.72 Å
5bB	5b	B^a	$P2_12_12_1$	56.0	59.5	70.0	90	90	90	67905/17395	3.6% 5.3% at 1.94 Å
5cB	5c	B^a	$P2_12_12_1$	56.8	59.3	68.8	90	90	90	60473/17412	5.7% 9.7% at 1.93 Å
6aC	6a	C^b	$P2_12_12_1$	46.6	118.9	143.7	90	90	90	185472/55717	8.5% 24% at 1.95 Å
6bC	6b	C^b	$P2_12_12_1$	46.6	119.3	143.9	90	90	90	163290/45438	5.4% 11.3% at 2.05 Å
6cD	6c	D^b	$I2_13$	125.6	125.6	125.6	90	90	90	88791/31947	8.6% 30.9% at 2.8 Å

^a Data collection on a Centronix (Siemens) area detector. ^b Data collection on an image plate (Mar Research) system.

Table 3. Refinement Statistics²⁶

compound/ crystal form	reflections (completeness %)	number of non hydrogen atoms per asymmetric unit				rms deviation		R_{fac} , %
		protein	ions	solvent	inhibitor	bond	angles	
3A	17689 (97.6)	1629 ^a	1 Ca ²⁺	201	28	0.006	1.372	16.66
3E	9225 (68.4)	1629 ^a	1 Ca ²⁺	95	28	0.006	1.354	17.82
4A	13577 (74.2)	1629 ^a	1 Ca ²⁺	153	38	0.006	1.291	17.27
5aA	19537 (91.2)	1629 ^a	1 Ca ²⁺	192	30	0.006	1.355	18.20
5aB	22002 (95.3)	1629 ^a	1 SO ₄ ²⁻	160	30	0.005	1.362	18.67
5bB	15556 (97.8)	1629 ^a	1 SO ₄ ²⁻	138	35	0.009	1.436	18.53
5cB	16668 (94.6)	1629 ^a	1 SO ₄ ²⁻	138	33	0.008	1.406	18.28
6aC	50786 (87.8)	6516 ^b	4 Ca ²⁺	591	192	0.007	1.377	17.46
6bC	43807 (92.2)	6516 ^b	4 Ca ²⁺	446	192	0.007	1.383	17.57
6cD	7217 (93.5)	1629 ^a	1 Ca ²⁺	72	43	0.006	1.283	18.08

^a Monomer per asymmetric unit. ^b Tetramer per asymmetric unit.

In each complex, the trypsin moieties show little variation, with rms deviations of C α atoms with respect to benzamide:trypsin (coordinates from Protein Data Bank code 1ppc) between 0.23 and 0.37 Å, within the experimental coordinate error estimated according to the method of Luzzati.²⁹ In the neighborhood of the specificity pocket, the only significant difference is in the orientation of the side chain of Gln192 at the entrance. In each of the orthorhombic **B** crystal forms, Gln192N ϵ^2 points toward a bound sulfate ion which appears to be coordinated by Ser195O γ , Gly193N, His57N ϵ^2 , and up to three bound water molecules (when not displaced by the inhibitor). This sulfate ion also appears to be present in the cubic form **D**, although the lower resolution of these data (2.8 Å) precludes its unequivocal identification; in this crystal form, the side chain of Gln192 is not a ligand for the putative sulfate ion. In the absence of sulfate, this position can be occupied by a Zn²⁺ ion, reflecting the amphiphilic nature of Ser195O γ and His57N ϵ^2 .³⁰

The electron densities obtained are sufficiently clear to characterize the binding mode of every inhibitor (Figures 2, 3, 5–7). With the exception of **4** and **6c**, racemic inhibitor mixtures were used for cocrystallization. In each case, however, the resulting densities indicate that for all the pseudo-peptidic inhibitors containing 3-amidinophenylalanine, the L-enantiomer was bound to trypsin, in contrast to the 4-amidinophe-

nylalanine derivative NAPAP where the D-enantiomer was found.^{12,14,15}

The individual binding modes of the various classes of inhibitors are described in detail below.

Binding of Compound 4. As inhibitor **4** binds to trypsin in a fashion very similar to that of the well-described 3-TAPAP (**2**)^{12,13} (Figure 2), we shall use this structure to illustrate some basic features of pseudo-peptidic inhibitor:serine proteinase complexes seen to date. The basic benzamidino function of the inhibitor is buried in the S1 specificity pocket. The amidino moiety makes a symmetric salt bridge with the carboxylate of Asp189 and is further stabilized by contacts to the carbonyl group of Gly219 and (via a bridging water molecule) to the hydroxyl group of Ser190. The solvent structure within the pocket is identical to that observed in the NAPAP:trypsin structure.^{12,13} Both the binding mode and solvent organization in the S1 pocket are conserved in all the structures described here (although the low resolution of **6cD** precludes location of the buried solvent molecules, residual electron density suggests that they are indeed present).

The following features, observed also for TAPAP (**2**),¹³ are shared by only some of the peptidic inhibitors described here. The “main chain” of the inhibitor runs antiparallel to trypsin segment Ser214–Ser217, forming a short β -ladder via hydrogen bonds between the central amidinophenylalananyl amide and carbonyl groups and

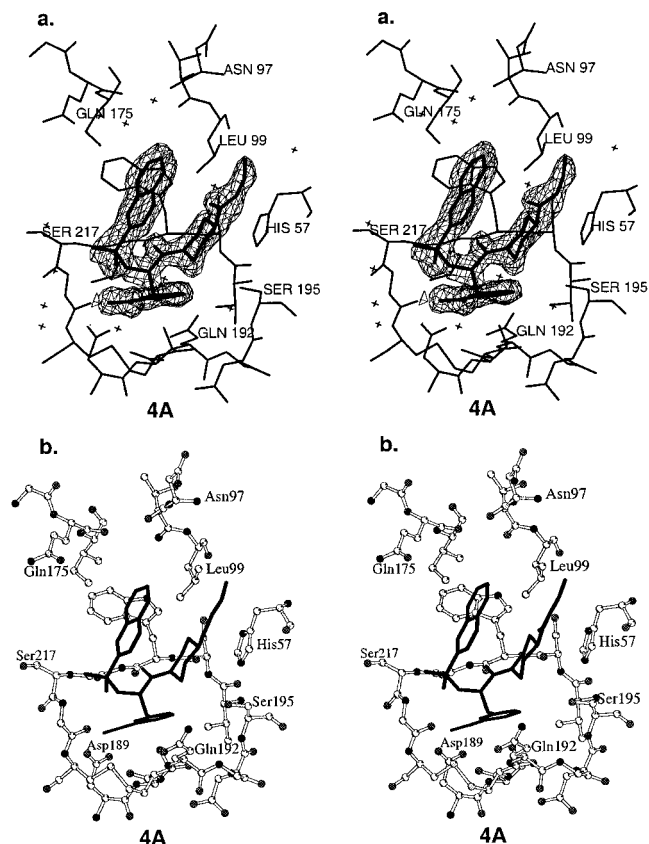


Figure 2. (a) Experimental electron density for compound **4A** in bovine trypsin.⁴¹ (b) Stereodiagram depicting the binding of **4A** (black) in bovine trypsin.⁴²

Gly216 O and N. The N-terminal naphthylsulfonyl group occupies the S3/S4 pocket, where the ring system is periplanar to the indole group of Trp215 and one of the two sulfonyl oxygens hydrogen bonds to Gly219N. The C-terminal piperidyl ethyl ester occupies the S2 pocket and is parallel to the naphthyl moiety and the imidazole portion of His57.

Binding of Compounds 6a–c. The binding mode of **6aC**, **6bC**, and **6cD** (Figure 3) is similar to that of **4A**. A superposition of the corresponding trypsin coordinates reveals negligible differences in the orientations of the benzamidine and piperazine/piperidide functionalities, and the short antiparallel β -sheet is formed between the main chain of the inhibitor and the segment Ser214–Ser217. Both sulfonyl oxygens of the N-terminal TIPPS moiety are directed toward Gly219N, with one making a hydrogen bond. The N-terminal ring system is perpendicular to the indole ring of Trp215, but in contrast to the N-terminal naphthyl group of compound **4**, the TIPPS moiety does not enter the S3/S4 pocket due to steric hindrance of the isopropyl groups (Figure 3d). The inhibitor juts out of the specificity pocket to expose its hydrophobic surface.

It seems likely that the prominent exposure of this large hydrophobic N-terminal group influenced crystal growth: the TIPPS residue connected to the α -nitrogen of the inhibitors **6a**, **6b**, and **6c** is too bulky to fit into the usual trigonal (A) or orthorhombic (B) crystal forms. Crystals containing these compounds took considerably longer to grow than the usual week or so for the A and B forms. **6a** and **6b** crystallized in a large orthorhombic space group (C), with a tetramer in the asymmetric unit.

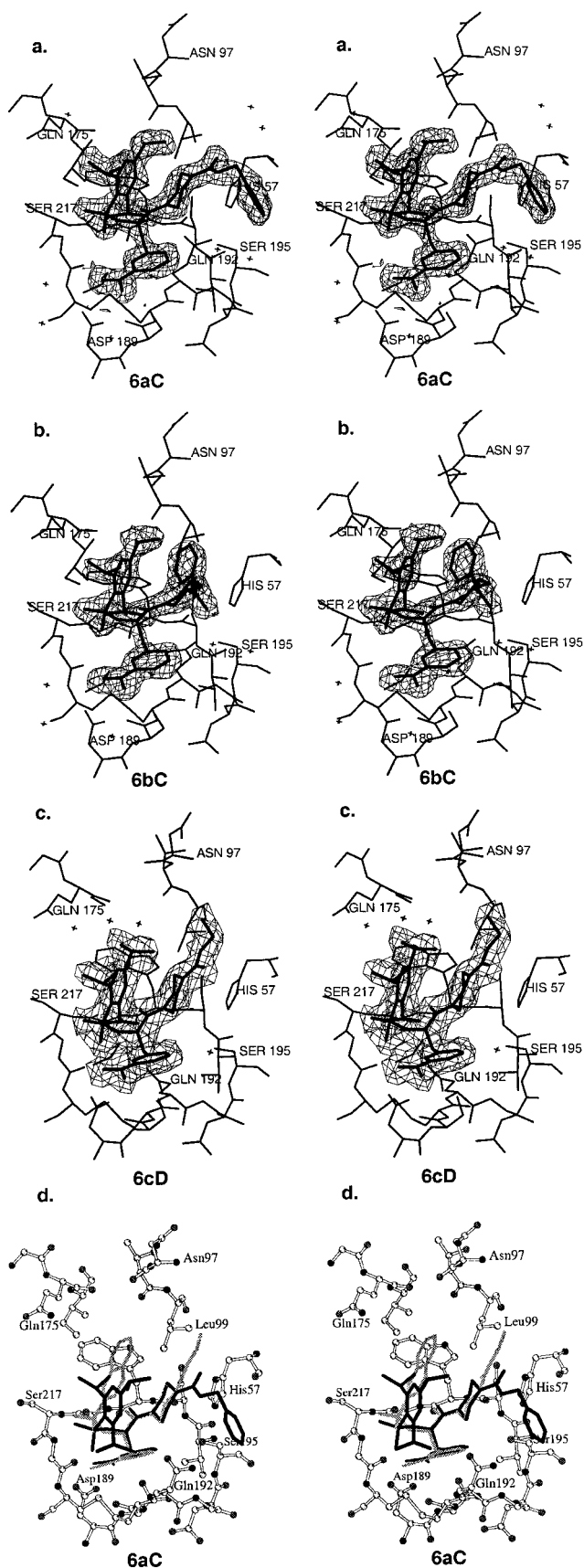


Figure 3. (a–c) Experimental electron densities for compounds **6aC**, **6bC**, and **6cD** (“TIPPS inhibitors”) in bovine trypsin.⁴¹ (d) Stereodiagram depicting the binding of **6aC** (black) in bovine trypsin, with **4A** overlaid (gray).⁴²

The active sites of two trypsin molecules face one another, with the inhibitor moieties making multiple

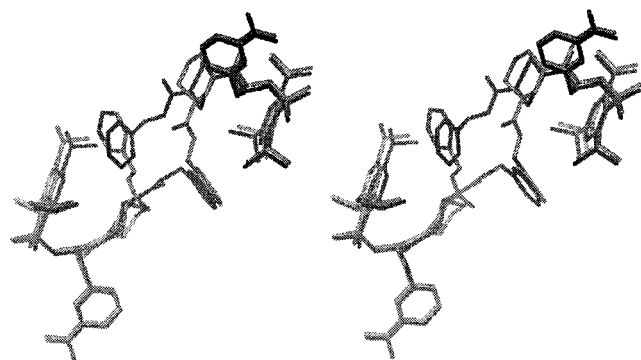


Figure 4. Superposition of **6aC** (dark) and **6bC** (light); the isomorphous trypsin moieties are not shown. The crystal packing for these two complexes are identical; in each case, the inhibitor molecule of one trypsin complex faces and contacts its local symmetry related mate. The C-terminal benzyl ester of **6a** (dark gray) contacts the TIPPS residue of the neighboring molecule, while the benzyl amide of **6b** (light gray) contacts its own TIPPS residue. As a result of this organization, the inhibitors are completely isolated from bulk solvent.⁴¹

interactions with their local symmetry related mates (Figure 4). The long C-terminal “arms” of the inhibitors wrap around the N-terminal TIPPS residue of the neighboring (**6aC**) or parent (**6bC**) inhibitor molecule, with the C-terminal benzyl groups of each inhibitor occupying the same spatial positions (Figure 4). The hydrophobic surfaces of the inhibitors are shielded completely from the bulk solvent. This shielding of the hydrophobic surface is presumably responsible for the observed dimerization in this crystal form.

A possible influence of crystal packing forces on the binding of this group of inhibitors could be ruled out after solution of the structure of **6cD** (Figure 3c). This inhibitor, which lacks the C-terminal aromatic function of **6a** and **6b**, cocrystallizes with trypsin in a novel cubic crystal form D where the inhibitor is freely accessible to the solvent. Superposition of **6cD** with **6aC** and **6bC** reveals identical binding modes for each of the TIPPS-containing compounds.

Binding of Compounds 5a–c. As described for **4**, the benzamidine moiety of this series occupies the S1 pocket, engaged in a salt bridge to Asp189. None of the other binding features described above is conserved, however. In contrast to the binding mode observed for **4**, these inhibitors do not form a β -sheet-like structure with Ser214–Ser217 nor do either of the sulfonyl oxygens approach Gly219N (Figure 5). The conformations observed for the N-terminal groups of these inhibitors are clearly influenced by crystal packing and are described separately.

Binding of Compound 5aA (trigonal, Figure 5a,e). The inhibitor exhibits an extended conformation, with the N-terminal tosyl group occupying the S3/S4 site, but does not run antiparallel to the segment Ser214–Ser217. Compared to **4**, fewer hydrogen bonds between the inhibitor and the enzyme backbone are observed; the only interaction of this kind is found between the carbonyl oxygen of the inhibitor glycine and Gly216N. The C-terminal methyl ester points away from the surface of the enzyme, not contributing to the binding but restricting the conformational space of Gln192. The conformational space of the inhibitor is also restricted

by the crystal packing, although no side chain rearrangements in neighboring molecules are necessary.

Binding of Compound 5aB (orthorhombic, Figure 5b,f). **5a** also adopts an extended conformation in this crystal packing, but neither runs antiparallel to Ser214–Ser217 nor makes multiple hydrogen bond interactions to the trypsin backbone. As a consequence of a different dihedral angle of the C^β – C^γ bond of the central phenylalanine moiety, the inhibitor main chain does not extend into the S3/S4 site as in **5aA**. It runs almost parallel to Ser217–Cys220, with the glycy spacer amide and carbonyl groups hydrogen bonding to Gly216O and Gly219N, respectively. The tosyl group points away from the enzyme, and occupies an hydrophobic depression on the surface of a symmetry-related molecule. This group apparently does not contribute to the binding of the inhibitor to trypsin.

Binding of Compounds 5bB, 5cB (orthorhombic, Figures 5c and 5d). The two inhibitors also exhibit an extended conformation, with the N-terminal naphthyl groups occupying the neighboring hydrophobic depression described for **5aB**. Although the N-terminal and glycy residues make no interactions less than 4 Å with the parent enzyme molecule, the dihedral angles describing the inhibitor structure resemble those of **5aA** more closely than **5aB**. The latter is perhaps surprising, considering that **5aB**, **5bB**, and **5cB** all exhibit the same crystal packing and hence the same immediate inhibitor environment. This in turn suggests that the inhibitor conformation observed for **5aA**, **5bB**, and **5cB** is nearer to that present when bound to trypsin in solution.

Binding of Compound 3. Compound **3** crystallized in two different crystal forms (**3A** and **3E**) and, in addition, was successfully soaked into the “open” orthorhombic form, where the active site is fully accessible from bulk solvent (data not shown) (Figure 6). Superposition of the three structures reveals negligible deviations; in the following, the structure of **3A** will be described as being the best resolved. The inhibitor exhibits an extended structure, with the “proximal” benzamidine function occupying the S1 specificity pocket as described for **4** (Figure 6c; see above). The “distal” benzamidine reaches out toward the S3/S4 pocket. In **3A**, the charge of the distal amidino group is compensated by (1) a hydrogen bond (2.8 Å) between one nitrogen and Asn97O, (2) a hydrogen bond (3.4 Å) between the second nitrogen to Gln175O^{e1}, and (3) by two solvent molecules which bridge to Gln175O and Thr96O. The hydrogen bond network is similar in the orthorhombic form (**3E**), but only one solvent molecule bridges to the carbonyl oxygens of Gln175 and Thr96. The cycloheptanone ring spacer makes no significant contacts to the enzyme, although its carbonyl oxygen approaches Gln192N^{e2}. The double bond connecting the proximal benzamidine to the cycloheptanone moiety adopts a *Z*-configuration while the double bond connecting the distal benzamidine to the central ring adopts an *E*-configuration.

Discussion

The Inhibition of Trypsin. We have investigated the binding modes of synthetic serine proteinase inhibitors in cocrystals of bovine trypsin. Inhibition constants for trypsin vary by 3 orders of magnitude for the

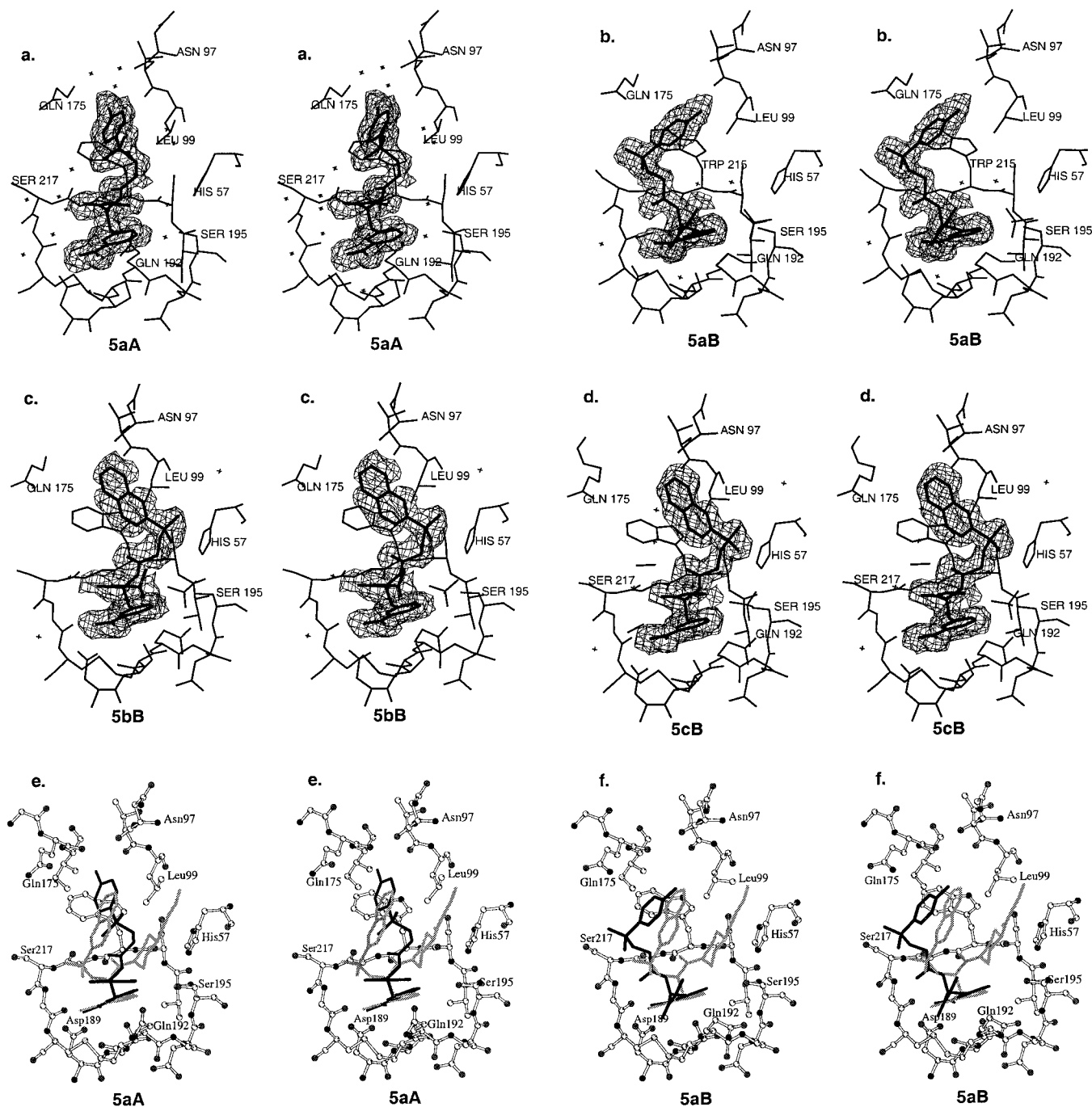


Figure 5. (a–d) Experimental electron densities for compounds **5aA**, **5aB**, **5bB**, and **5cB** in bovine trypsin.⁴¹ (e, f) Stereodiagrams depicting the binding of (e) **5aA** and (f) **5aB** (black) in bovine trypsin, with **4A** overlaid (gray).⁴²

compounds used in this study (**5c** $K_i = 9.2 \mu\text{M}$, **4** $K_i = 0.0084 \mu\text{M}$, see Table 1). The structures allow us to rationalize this variation as follows. The inhibitors realize a combination of ionic and hydrophobic interactions in the S1 pocket (I1), a combination of hydrophobic interactions in the S2 (I2) and S3/S4 pockets (I3), hydrogen bonds with the protein segment 214–220 at different sites (I4), and electrostatic interactions in the back of the S3/S4 pocket (I5) (Figure 7).

All inhibitors share the basic benzamidino moiety, which binds into the S1 pocket. A K_i value below that of benzamide (~10 μM for trypsin) indicates an effect of interactions outside the S1 pocket. Thus, the 10^{-5} to 10^{-6} M inhibition constants for inhibitors **5a**, **5b**, and **5c** indicate a predominantly benzamide-based inter-

action, with little or no role for groups outside I1, explaining the diverse structural results for this class.

In contrast, compound **4** uses additional docking sites for the interaction with trypsin: hydrophobic interactions at I2 and I3 and hydrogen bonds at I4, lowering the K_i value by 4 orders of magnitude. Although difficult to quantify, the isolated influence of each kind of interaction can be estimated by comparison of different inhibitors as follows (Figure 7; Table 4).

Substitution at the C-terminal group alters the binding significantly: An unsubstituted piperazine instead of the piperidine (as in compound **4**) leads to a higher K_i value,⁸ probably due to unfavorable interactions between the basic amide of the piperazine moiety and the imidazole side chain of His57. Substitutions at

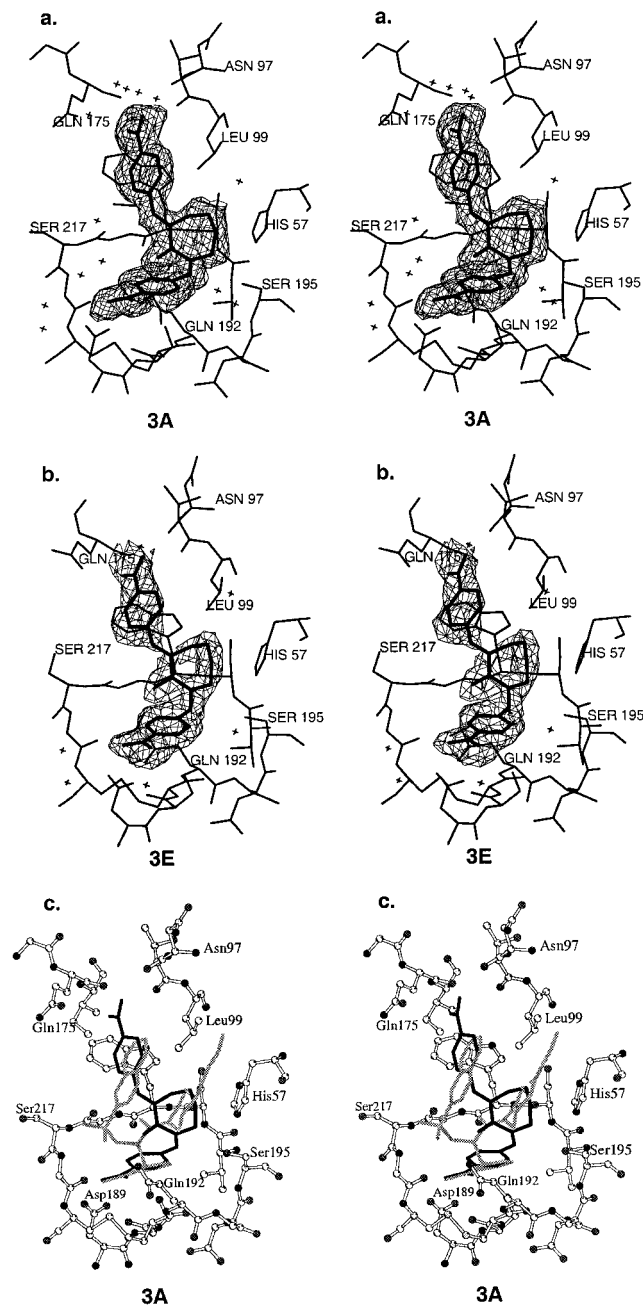


Figure 6. (a, b) Experimental electron densities for compound **3A** and **3E** in bovine trypsin.⁴¹ (c) Stereodiagram depicting the binding of **3A** (black) in bovine trypsin, with **4A** overlaid (gray).⁴²

position 3 of the piperidine (as in **6b**) have little effect on the K_i .⁷ In contrast, substitutions at position 4 of the piperidine or piperazine moiety can enhance the affinity considerably.^{7,8} Although no strong interactions could be observed, the coalescence of the branched aliphatic chain of Leu99 and the ethyl ester ("hydrophobic forces") might play a role in the strong inhibition observed for compound **4**.

The nature of the N-terminal protecting group (interaction I3) also plays a role (Table 5). Comparing inhibitors with a 4-methyl piperidide C-terminal group,⁷ an unsubstituted or Boc-substituted N-terminus results in a 10^{-5} M inhibition for trypsin. Substitution of the N-terminal group with tosyl, naphthyl, or TIPPS residues results in 10^{-7} M trypsin inhibition, while replace-

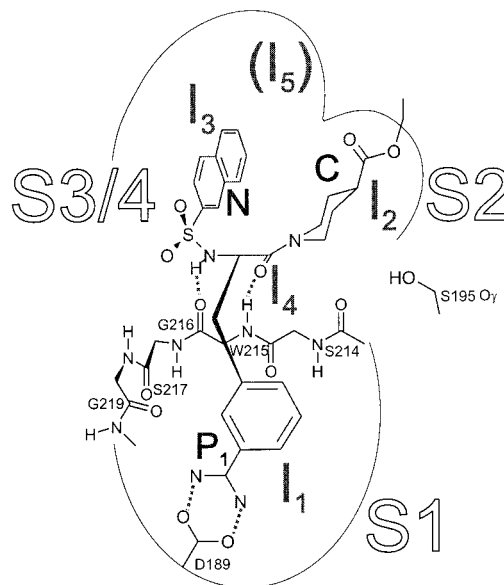


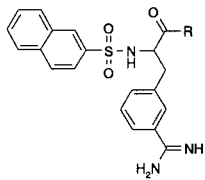
Figure 7. Schematic representation of the binding mode of the benzamidine type inhibitors using compound **4** as example. Inhibitor **4** consists of three parts: the 3-amidino-phenylalanine residue (**P1**), the C-terminal group isonipecotic acid ethylester (**C**), and the N-terminal group naphthylsulfonyl moiety (**N**). **P1** binds into the S1 pocket, where it makes both hydrophilic and ionic interactions (interaction site I1). The C-terminal group forms mostly hydrophobic interactions with the S2 pocket (interaction site I2), and the N-terminal group forms similar interactions with the S3/S4 pocket (interaction site I3). The short antiparallel β -sheet between the main chain atoms of P1 and Trp215/Gly216 is called interaction site I4. The binding of **4** does not utilize the electrostatic interaction I5.

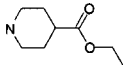
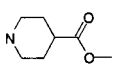
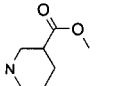
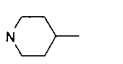
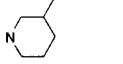
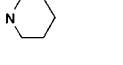
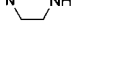
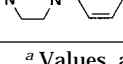
ment with the less hydrophobic yet bulkier anthrachinone moiety yields a 10^{-8} M K_i value against trypsin,⁷ suggesting that trypsin favors a bulky group in this position. As trypsin does not appear to possess any particular active groups in this region, the driving force behind this improvement in affinity is not clear.

Compounds of the type **6** exhibit an unexpected binding mode, with a large hydrophobic surface that is exposed to solvent. The low K_i values of these compounds are therefore striking, in particular as there appear to be few close contacts between the enzyme and inhibitor. In addition to interactions I1, I2, and I4, interaction I3 is realized with only one of the isopropyl groups of the TIPPS moiety in the S3/S4 pocket. The lack of directed specific interactions explains why this series of compounds is relatively unspecific, binding with roughly equal affinity to each of the different enzymes under study (Table 1).

The binding mode of compound **3** is of a completely different nature, in that the inhibitor occupies interaction sites I1, I2, and I3, but does not hydrogen bond to the backbone segment 216–220 (I4). The distal aromatic ring of **3** superimposes well on the N-terminal ring systems of **2** and **4**. The loss of interaction I4 is evidently compensated by the introduction of additional electrostatic interactions at I5.

Trypsin as a Model System. With these structures in hand, we can attempt to explain the observed variation in selectivity of these compounds against the serine proteinases factor Xa, tPA, and uPA (Figures 8 and 9). Before applying these results to the inhibition

Table 4. Dissociation Constants K_i (μM) for Inhibition of Bovine Trypsin, Bovine Thrombin, Bovine Factor Xa, and Human uPA by Piperidides and Piperazines of β -Naphthylsulfonylated 3-Amidino-D,L-Phenylalanine^{7,8 a}


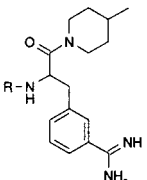
R	Trypsin	factor Xa	thrombin	uPA
 (4*)	0.0084	18	0.22	4.5
	0.036	43	0.017	9.3
	0.39	18	0.15	26
	0.14	41	0.0062	31
	0.53	32	0.13	35
	0.33	38	0.065	38
	0.22	21	0.50	48
	0.027	27	0.52	41

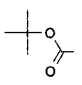
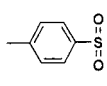
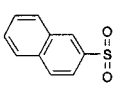
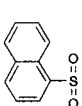
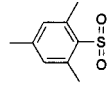
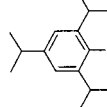
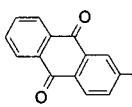
^a Values are for D,L-racemates except those denoted by an asterisk (*), where the pure L-enantiomer was measured.

of the target enzymes, it is important to discuss the validity of such an approach.

Comparison of the Binding of One Inhibitor to the Same Target Enzyme in Different Crystal Forms Reveals the Effects of Crystal Packing. For compound **3**, there is little influence of crystal packing on the observed binding mode in two different crystal forms (A and E). The same conformation is also observed in the "open" orthorhombic form, where the active site is fully accessible from bulk solvent (data not shown). We have also shown previously that there are negligible differences in the binding modes of the DX9065a series of factor Xa inhibitors to trypsin in different crystal environments.²⁰

On the other hand, crystal contacts clearly influence the binding modes seen for structures **5aA**, **5aB**, **5bB**, **5cB**, **6aC**, and **6bC**. Resolution of the structure **6cD** confirmed the binding mode observed for **6aC** and **6bC**. For inhibitors **5a**, **5b**, and **5c**, however, the situation is more complex. These very similar compounds exhibit two different binding modes in two different crystal forms. As structure **5aA** shows the most protein–ligand

Table 5. Dissociation Constants K_i (μM) for Inhibition of Bovine Trypsin, Bovine Thrombin, Bovine Factor Xa, and Human uPA by 4-Methylpiperidides of β -Naphthylsulfonylated 3-Amidino-D,L-Phenylalanine^{7,8 a}


R	Trypsin	factor Xa	thrombin	uPA
H	29	230	27	800
	14	64	1.2	56
	0.52	71	0.026	25
	0.14	41	0.0062	31
	0.63	42	0.016	34
	4.0	95	0.059	16
	0.69	2.0	0.075	2.0
	0.074	2.3	0.026	40

^a Values are for D,L-racemates except those denoted by an asterisk (*), where the pure L-enantiomer was measured.

contacts and **5bB** and **5cB** in the other space group can be more easily rearranged to the binding mode of **5aA** than to that of **5aB**, we believe structure **5aA** to be representative of a productive binding mode. The fact that **5a** shows two distinct binding modes suggests that 10^{-5} M represents the upper K_i limit for trypsin for this approach (corresponding to the K_i for benzamidine alone).

Comparison of the Binding of One Inhibitor to Different Target Enzymes Reveals the Validity of Trypsin as a Model System. The binding modes of NAPAP (**1**) in complex with trypsin¹² and thrombin,¹⁵ DX9065a in complex with trypsin²⁰ and factor Xa,²¹ and **3** in trypsin [this work] and tPA³¹ are in each case highly similar. Minor changes occur in the orienta-

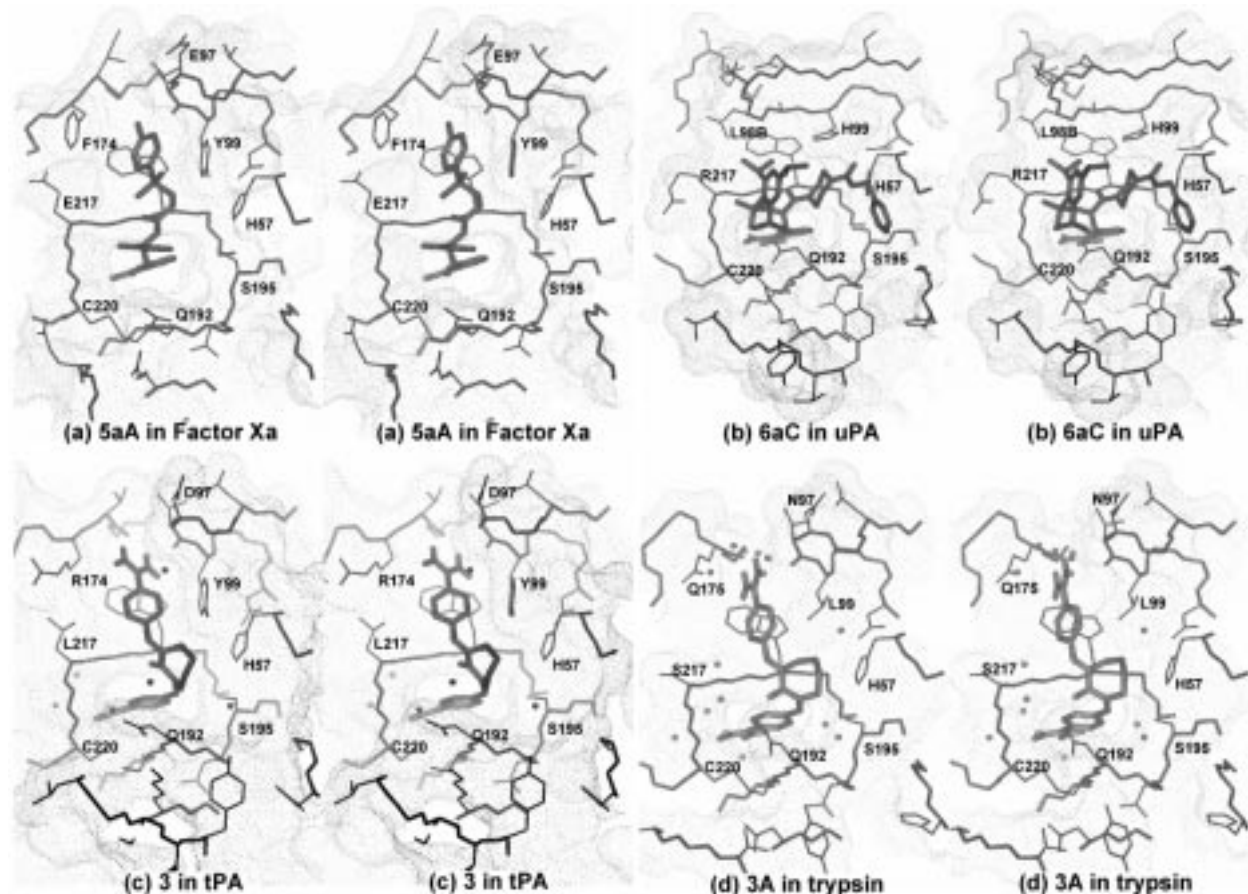


Figure 8. Stereoviews comparing the binding modes of (a) **5aA** transferred to the active site of factor Xa, (b) **6aC** transferred to the active site of uPA, (c) **3** in complex with human tPA,³¹ and (d) **3A** in complex with bovine trypsin.⁴¹

tions of individual inhibitor moieties, such as seen for the distal aromatic ring of **3** (see below and Figure 8c,d). Further differences are seen in the solvent organization and, surprisingly, in the disposition of the Asp189 carboxylate to the inhibitor amidino function, which does not always make symmetric salt bridges.²¹ Nevertheless, the structures seen in trypsin to date have proven reliable for a qualitative interpretation of the SARs.

The Inhibition of Factor Xa and tPA. Transfer of compound **3** into the active site of factor Xa reveals the same three-point interaction previously described for DX9065a:^{20,21} (1) salt bridge formation between the proximal benzamidino function and Asp189 (interaction I1), (2) burial of the distal aromatic ring in the hydrophobic box delineated by Tyr99, Phe174, and Trp215 (interaction I3), and (3) concomitant electrostatic interactions between the distal amidino function and the "cation hole" of factor Xa formed by the carbonyl groups of Glu97, Thr98, and Ile175 (interaction I5). Support for this mode is given by the structure of the same inhibitor in complex with tPA³¹ (Figure 8c), which exhibits a very similar interaction surface (Tyr99, Thr98, and Asp97) (Figure 9). The high resolution of the trypsin data allow the location of solvent molecules that mediate the electrostatic interaction between the distal amidino function and the carbonyl groups in the cation hole.

The high-resolution data also allow the unambiguous identification of the bound compound **3** as the *E,Z*-isomer, allowing simultaneous occupation of the S1

pocket by the proximal benzamidine and the S3/S4 pocket by the distal benzamidine. A definitive measurement of the dihedral angles of the tPA-bound conformer was not possible at the observed resolution,³¹ although the electron density in tPA is consistent with a *Z*-configuration for the double bond connecting the proximal benzamidine to the cycloheptanone moiety. In tPA, the cycloheptanone moiety of the compound is rotated relative to the conformation in trypsin, thereby preventing unfavorable interactions between the inhibitor and Tyr99. As a consequence, the conformation of the distal double bond is shifted toward the *Z*-configuration. This correlates with the recent finding that the *Z,Z*-isomer is active against factor Xa.³²

Superposition of compound **3** in trypsin and tPA indicates a 45° rotation of the distal aromatic ring, such that it becomes parallel to Trp215 and perpendicular to Tyr99 (Figure 8c,d). Judging by the improved inhibition of tPA by **3** compared to trypsin, this constellation of aromatics should be energetically favorable. The addition of a further perpendicular aromatic group, presented by Phe174 in factor Xa, could result in the higher affinity for factor Xa over tPA. Such a ring reorientation is also observed for the central aromatic ring of DX9065a when the trypsin- and factor Xa-bound conformations are compared.^{20,21}

Inhibition of factor Xa by **5a**, **5b**, and **5c** can be rationalized if one assumes the binding mode observed for **5aA** (Figure 8a). In contrast to the compact form presented by **4**, the extended conformation of these

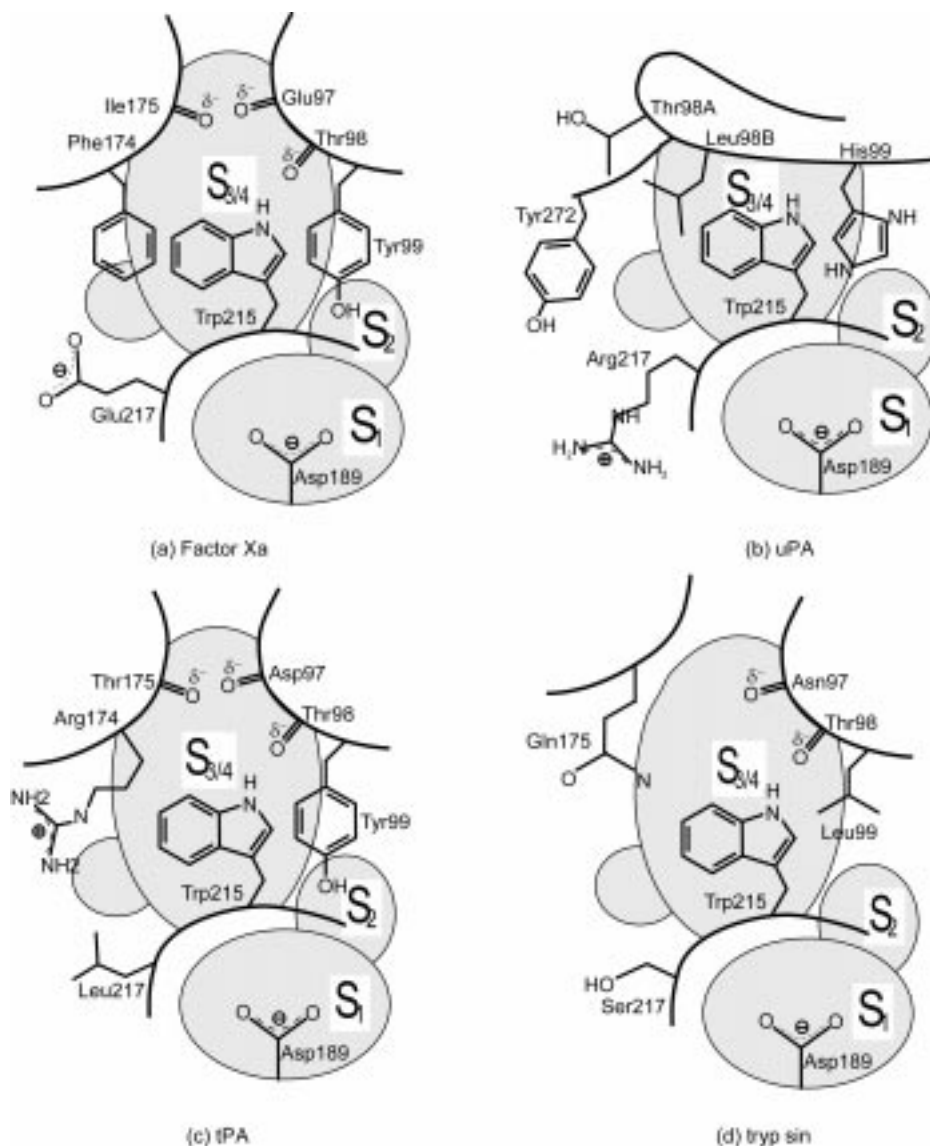


Figure 9. Schematic representations of the active sites of (a) factor Xa, (b) uPA, (c) tPA,³¹ and (d) trypsin.

inhibitors allows simultaneous occupation of the S1 pocket by the benzamidine function (I1) and the hydrophobic S3/S4 pocket by the tosyl or naphthylsulfonyl *N*-terminal group (I3). This is at the expense of favorable polar interactions (such as the antiparallel β -sheet formation (I4) observed for NAPAP (**1**) and TAPAP (**2**) type inhibitors). The two-point interaction (comprising electrostatic interactions in the S1 pocket and hydrophobic interactions in the S3/S4 pocket) may explain the selectivity of this class of compounds for factor Xa over tPA. With its three-membered hydrophobic box (Figure 9), factor Xa is well suited to binding hydrophobic groups. In contrast, the S3/S4 pocket in tPA is bordered on one side by Arg174 (Phe174 in factor Xa) (Figure 9), making this pocket less hydrophobic.

The interactions described here provide experimental support for the relevance of the hydrophobic box and the cation hole in the design of factor Xa specific inhibitors.^{20,21} These regions have recently been utilized in modeling studies in the formulation of novel nonpeptidic inhibitors incorporating a second basic group³³ or hydrophobic group.³⁴ As a result of the structural similarities in S3/S4 between factor Xa and tPA outlined above, however, compounds utilizing the hydrophobic

box alone may be superior due to a better selectivity against tPA.

The Inhibition of Urokinase. Despite its importance as a possible target in cancer treatment, few examples of uPA inhibitors are available in the literature.^{35–37} As observed above, specific high-affinity inhibition of trypsin-like serine proteinases can be achieved in most cases through optimal occupation of the S2/S3/S4 pockets. In uPA, these pockets are not available, being eclipsed by His99 (S2) and the 99-loop (S3/S4) (Figure 9). Thus, binding of compounds **1–5** would be hindered sterically in uPA in the conformations presented here. Inhibitors for uPA must make use of alternative binding determinants.

Due to the 2-substituted isopropyl group of the TIPPS residue, compounds **6a–6c** do not enter the S3/S4 site (Figure 8b). This lack of unfavorable interactions leads to the improved relative inhibition of these compounds toward uPA and to the reduced selectivity against related proteinases such as factor Xa, trypsin, and tPA. Simultaneous hydrophobic burial of Leu98B by the 2-isopropyl group, hydrogen bond formation between the sulfonyl group and Gly219N, and possible hydrogen bonding between the C-terminal carbonyl group and

His99 could enhance the interaction, resulting in the improved inhibition of **6c**. Clearly, compound **4** could also adopt the uPA binding mode; compared to compounds **6a–6c**, however, **4** would lack the hydrophobic burial component, explaining the reduced inhibitory activities of **4** for uPA.

The relatively low K_i of **3** for uPA is particularly interesting, as this compound would not be able to bind to uPA in the conformation observed in trypsin or tPA. It is conceivable that compound **3** binds with the distal benzamidine oriented toward the 148-loop of uPA. Such a binding mode has been seen for a related bis-benzamidine inhibitor in trypsin³⁸ and has been proposed for inhibitors of the tetrameric serine proteinase trypsinase.³⁹ In uPA, however, there are no residues in this region capable of compensating for the positive charge of the distal amidino group. The possibility that potent uPA inhibitors might bind to specific docking sites on the 148-loop cannot be excluded, especially as this loop might undergo structural rearrangements upon ligand binding.

Conclusions

The structures reported in this paper provide a rationale for the selectivity of benzamidine-based inhibitors for various members of the trypsin-like serine proteinase superfamily. We have shown that trypsin provides a functional model system for the analysis of protein–ligand interactions within this class. As we noted earlier, however,²⁰ such structural information presents only a partial picture of the inhibition process. The X-ray crystal structures presented here fail to deliver any information on the kinetics and thermodynamics of the reaction. In particular, entropic effects are overlooked—for example, an inhibitor that in solution already possesses the conformation observed when bound to the enzyme has a considerable entropic advantage over either a flexible inhibitor or one that must undergo rearrangement on binding to the target protein. In this way, it is possible to envisage that inhibitors **1**, **2**, **4**, and **6** fold around their hydrophobic cores (hydrophobic collapse of the N- and C-terminal groups in Figure 7) in solution, providing them with an entropic advantage over compounds of the type **3** and **5**. Again, the rigid inhibitor **3** has only a few degrees of freedom, while the relatively hydrophilic class **5** inhibitors could adopt multiple conformations in solution—reflected in the differing conformations observed in this paper. Similarly, we are unable to ascertain the role of ligand and receptor solvation and of the different kinetic pathways taken for shedding bound water molecules (desolvation).

These aspects are, of course, also a problem in all structure-based modeling approaches. Notwithstanding the obvious limitations of carrying out such experiments in trypsin, this semiconservative approach provides a useful link between the “real” and the “modeling” worlds. Indeed, the inhibition mode displayed by the TIPPS-containing compounds (**6**), which exhibit reasonable affinity despite presenting an extremely hydrophobic surface toward the bulk solvent, reveals a fundamental lack of understanding of the processes governing such protein–ligand interactions and is clearly a subject for further study.

X-ray crystallographic investigations of inhibitors in complex with trypsin represent a feasible method for the identification of important interaction sites in proteinases not amenable to routine crystallization. The advantages of this approach (high resolution, reproducible crystallization conditions, fast turnover) greatly outweigh the disadvantages (such as alternative binding modes), providing a reliable starting point for the design of novel compounds.⁴⁰

Acknowledgment. We are grateful to P. Wikström and H. Vieweg of Pentapharm Ltd. (Basel, Switzerland) for the synthesis of compounds used in this study.

References

- (1) Abbreviations: tPA, tissue-type plasminogen activator; uPA, urokinase; SAR, structure–activity relationship; NAPAP, *N*²-(2-naphthylsulfonylglycyl)-4-amidino-D,L-phenylalanine-piperidine; 3-TAPAP, *N*²-tosyl-3-amidino-D,L-phenylalanine-piperidine; TIPPS, 2,4,6-triisopropylphenylsulfonyl; rms, root-mean-square.
- (2) Harker, L. A.; Hanson, S. R.; Kelly, A. B. Antithrombotic strategies targeting thrombin activities, thrombin receptors and thrombin generation. *Thromb. Haemost.* **1997**, *78*, 736–741.
- (3) Andreassen, P. A.; Kjoller, L.; Christensen, L.; Duffy, M. J. The urokinase-type plasminogen activator system in cancer metastasis – A review. *Int. J. Cancer* **1997**, *72*, 1–22.
- (4) Rabbani, S. A.; Xing, R. H. M. Role of urokinase (uPA) and its receptor (uPAR) in invasion and metastasis of hormone-dependent malignancies. *Int. J. Oncol.* **1998**, *12*, 911–920.
- (5) Stürzebecher, J.; Markwardt, F.; Voigt, B.; Wagner, G.; Walsmann, P. Cyclic amides of *N*²-arylsulfonylaminoacylated 4-amidinophenylalanine – tight binding inhibitors of thrombin. *Thromb. Res.* **1983**, *29*, 635–642.
- (6) Stürzebecher, J.; Stürzebecher, U.; Vieweg, H.; Wagner, G.; Hauptmann, J.; Markwardt, F. Synthetic inhibitors of bovine factor Xa and thrombin. Comparison of their anticoagulant efficiency. *Thromb. Res.* **1989**, *54*, 245–252.
- (7) Stürzebecher, J.; Prasa, D.; Wikström, P.; Vieweg, H. Structure–activity relationships of inhibitors derived from 3-amidinophenylalanine. *J. Enzyme Inhib.* **1995**, *9*, 87–99.
- (8) Stürzebecher, J.; Prasa, D.; Hauptmann, J.; Vieweg, H.; Wikström, P. Synthesis and structure–activity relationships of potent thrombin inhibitors: piperazines of 3-amidinophenylalanine. *J. Med. Chem.* **1997**, *40*, 3091–3099.
- (9) Stürzebecher, J.; Markwardt, F.; Wagner, G.; Walsmann, P. Synthetische Hemmstoffe der Serinproteasen. 13. Quantitative Struktur-Wirkungs-Beziehungen bei der Hemmung von Trypsin, Plasmin und Thrombin durch 4-Amidinophenylverbindungen mit Ketonstruktur. [Synthetic inhibitors of serine proteinases. 13. Quantitative structure–activity relationship for inhibition of trypsin and thrombin by 4-amidinophenyl compounds with a ketone structure.] *Acta Biol. Med. Ger.* **1976**, *35*, 1665–1676.
- (10) Bode, W.; Mayr, I.; Baumann, U.; Huber, R.; Stone, S. R.; Hofsteenge, J. The refined 1.9 Å crystal structure of human alpha-thrombin: interaction with D-Phe-Pro-Arg chloromethylketone and significance of the Tyr-Pro-Pro-Trp insertion segment. *EMBO J.* **1989**, *8*, 3467–3475.
- (11) Stubbs, M. T.; Bode, W. Crystal structures of thrombin and thrombin complexes as a framework for antithrombotic drug design. *Perspect. Drug Discovery Des.* **1993**, *1*, 431–452.
- (12) Bode, W.; Turk, D.; Stürzebecher, J. Geometry of binding of the benzamidine- and arginine-based inhibitors NAPAP and MQPA to human α -thrombin. X-ray crystallographic determination of the NAPAP–trypsin complex and modeling of NAPAP–thrombin and MQPA–thrombin. *Eur. J. Biochem.* **1990**, *193*, 175–182.
- (13) Turk, D.; Stürzebecher, J.; Bode, W. Geometry of binding of the *N*²-tosylated piperidides of m-amidino, p-amidino- and p-guanidino phenylalanine to thrombin and trypsin. X-ray crystal structures of their trypsin complexes and modeling of their thrombin complexes. *FEBS Lett.* **1991**, *287*, 133–138.
- (14) Banner, D. W.; Hadvary, P. Crystallographic analysis at 3.0 Å resolution of the binding to human thrombin of four active site-directed inhibitors. *J. Biol. Chem.* **1991**, *266*, 20085–20093.
- (15) Brandstetter, H.; Turk, D.; Hoeffken, H. W.; Grosse, D.; Stürzebecher, J.; Martin, P. D.; Edwards, B. F.; Bode, W. Refined 2.3 Å X-ray crystal structure of bovine thrombin complexes formed with the benzamidine and arginine-based thrombin inhibitors NAPAP, 4-TAPAP and MQPA. A starting point for improving antithrombotics. *J. Mol. Biol.* **1992**, *226*, 1085–1099.
- (16) Padmanabhan, K.; Padmanabhan, K. P.; Tulinsky, A.; Park, C. H.; Bode, W.; Huber, R.; Blankenship, D. T.; Cardin, A. D.; Kisiel, W. Structure of human des(1–45) factor Xa at 2.2 Å resolution. *J. Mol. Biol.* **1993**, *232*, 947–966.

- (17) Lamba, D.; Bauer, M.; Huber, R.; Fischer, S.; Rudolph, R.; Kohnert, U.; Bode, W. The 2.3 Å crystal structure of the catalytic domain of recombinant two-chain human tissue-type plasminogen activator. *J. Mol. Biol.* **1996**, *258*, 117–135.
- (18) Spraggon, G.; Phillips, C.; Nowak, U.K.; Ponting, C. P.; Saunders, D.; Dobson, C. M.; Stuart, D. I.; Jones, E. Y. The crystal structure of the catalytic domain of human urokinase-type plasminogen activator. *Structure* **1995**, *3*, 681–691.
- (19) Stubbs, M. T. Structural aspects of Factor Xa Inhibition. *Curr. Pharm. Des.* **1996**, *2*, 543–552.
- (20) Stubbs, M. T.; Huber, R.; Bode, W. Crystal structures of factor Xa specific inhibitors in complex with trypsin: structural grounds for inhibition of factor Xa and selectivity against thrombin. *FEBS Lett.* **1995**, *375*, 103–107.
- (21) Brandstetter, H.; Kühne, A.; Bode, W.; Huber, R.; von der Saal, W.; Wirthensohn, K.; Engh, R. A. X-ray structure of active site-inhibited clotting factor Xa. Implications for drug design and substrate recognition. *J. Biol. Chem.* **1996**, *271*, 29988–29992.
- (22) Schroeder, D. D.; Shaw, E. Chromatography of trypsin and its derivatives. Characterization of a new active form of bovine trypsin. *J. Biol. Chem.* **1968**, *243*, 2943–2949.
- (23) Leslie, A. G. W. *Mosflm user guide, Mosflm version 5.20*; MRC Laboratory of Molecular Biology: Cambridge, U.K., 1994.
- (24) Kabsch, W. Automatic indexing of rotation diffraction patterns. *J. Appl. Crystallogr.* **1988**, *21*, 67–71.
- (25) Navaza, J. AMoRe: an automated package for molecular replacement. *Acta Crystallogr.* **1994**, *A50*, 157–163.
- (26) To distinguish the various structures, each inhibitor is described by the compound number given in Figure 1, together with a capital letter suffix for the space group as given in Table 2.
- (27) Brünger, A. *X-PLOR (Version 3.1). A System for X-ray Crystallography and NMR*; Yale University Press: New Haven, CT, 1992.
- (28) Jones, T. A.; Zou, J. Y.; Cowan, S. W.; Kjeldgaard, M. Improved methods for building protein models in electron density maps and location of errors in these models. *Acta Crystallogr.* **1991**, *47*, 110–119.
- (29) Luzzati, P. V. Traitement statistique des erreurs dans la détermination des structures cristallines. [A statistical treatment of errors in crystallographic structure determination.] *Acta Crystallogr.* **1952**, *5*, 802–810.
- (30) Katz, B. A.; Clark, J. M.; Finer-Moore, J. S.; Jenkins, T. E.; Johnson, C. R.; Ross, M. J.; Luong, C.; Moore, W. R.; Stroud, R. M. Design of potent selective zinc-mediated serine proteinase inhibitors. *Nature* **1998**, *391*, 608–612.
- (31) Renatus, M.; Bode, W.; Huber, R.; Stürzebecher, J.; Prasa, D.; Fischer, S.; Kohnert, U.; Stubbs, M. T. Structural mapping of the active site specificity determinants of human tissue-type plasminogen activator. *J. Biol. Chem.* **1997**, *272*, 21713–21719.
- (32) Shaw, K. J.; Guilford, W. J.; Dallas, J. L.; Koovakkaat, S. K.; McCarrick, M. A.; Liang, A.; Light, D. R.; Morrissey, M. M. (Z,Z)-2,7-bis(4-amidinobenzylidene)cycloheptan-1-one: Identification of a highly active inhibitor of blood coagulation Factor Xa. *J. Med. Chem.* **1998**, *41*, 3551–3556.
- (33) Maduskie, T. P. Jr.; McNamara, K. J.; Ru, Y.; Knabb, R. M.; Stouten, P. F. W. Rational design and synthesis of novel, potent bis-phenylamidine carboxylate factor Xa inhibitors. *J. Med. Chem.* **1998**, *41*, 53–62.
- (34) Klein, S. I.; Czekaj, M.; Gardner, C. G.; Guertin, K. R.; Cheney, D. L.; Spada, A. P.; Bolton, S. A.; Brown, K.; Colussi, D.; Heran, C. L.; Morgan, S. R.; Leadley, R. J.; Dunwiddie, C. T.; Perrone, M. H.; Chu, V. Identification and initial structure–activity relationships of a novel class of non peptide inhibitors of blood coagulation factor Xa. *J. Med. Chem.* **1998**, *41*, 437–450.
- (35) Stürzebecher, J.; Markwardt, F. Synthesische Inhibitoren der Serinproteinasen. 17. Einfluss von Benzamidinderivaten auf die Aktivität der Urokinase und den Ablauf der Fibrinolyse. [Synthetic inhibitors of serine proteinases. 17. The effect of benzamide derivatives on the activity of urokinase and the reduction of fibrinolysis.] *Pharmazie* **1978**, *33*, 599–602.
- (36) Towle, M. J.; Lee, A.; Maduakor, E. C.; Schwartz, C. E.; Bridges, A. J.; Littlefield, B. A. Inhibition of urokinase by 4-substituted benzo[b]thiophene-2-carboxamides: An important new class of selective synthetic urokinase inhibitor. *Cancer Res.* **1993**, *53*, 2553–2559.
- (37) Yang, H.; Henkin, J.; Kim, K. H.; Greer, J. Selective inhibition of urokinase by substituted phenylguanidines: Quantitative Structure–Activity relationship analyses. *J. Med. Chem.* **1990**, *33*, 2956–2961.
- (38) von der Saal, W.; Engh, R. A.; Eichinger, A.; Kuczniarz, R.; Sauer, J. Syntheses and selective inhibitory activities of terphenyl-bisamidines for serine proteases. *Arch. Pharm. Pharm. Med. Chem.* **1996**, *329*, 73–82.
- (39) Stubbs, M. T.; Morenweiser, R.; Stürzebecher, J.; Bauer, M.; Bode, W.; Huber, R.; Piechottka, G. P.; Matschiner, G.; Sommerhoff, C. P.; Fritz, H.; Auerswald, E. A. The three-dimensional structure of recombinant leech-derived trypsin inhibitor in complex with trypsin: Implications for the structure and function of human mast cell trypsinase and its inhibition. *J. Biol. Chem.* **1997**, *272*, 19931–19937.
- (40) Gabriel, B.; Stubbs, M. T.; Bergner, A.; Hauptmann, J.; Bode, W.; Stürzebecher, J.; Moroder, L. Structure-based design of benzamidine-type inhibitors of factor Xa. *J. Med. Chem.* **1998**, *41*, 4240–4250.
- (41) Figure prepared using the program MAIN (Turk, D. Weiterentwicklung eines Programmes für Molekülgraphik und Elektronendichte-Manipulation und seine Anwendung auf verschiedene Protein-Strukturaufklärungen. Ph.D. Thesis, Technische Universität München, 1992).
- (42) Figure prepared using the program MOLSCRIPT (Kraulis, P. MOLSCRIPT: a program to produce both detailed and schematic plots of protein structures. *J. Appl. Crystallogr.* **1991**, *24*, 946–950).

JM981068G